Rotation-invariant pattern matching using color ring projection

D. M. Tsia and Y. H. Tsai
Machine Vision Lab.
Department of Industrial Engineering and Management
Yuan-Ze University, Chung-Li, Taiwan, R.O.C.
E-mail: iedmtsai@saturn.yzu.edu.tw

1. INTRODUCTION

Template matching has been a popular and easily-implemented method for object detection [1], OCR [2] and PCB inspection [3]. It finds a pattern in the scene image by sliding the window of a reference template in a pixel-by-pixel basis, and computing the degree of similarity between them, in which the measure of similarity is commonly given by correlation or normalized correlation [4].

Pixel-by-pixel template matching is very time-consuming. For an input image of width N, and the template of width W, the computational complexity is in the order of $W^2 \cdot N^2$, given that the object orientations in both images to be matched are coincident. When we search an object with unknown orientation, the straightforward way to do template matching is to rotate the reference template in every possible orientation. The exhaustive template matching is extremely computation-intensive, and becomes impractical when arbitrary rotation is present. In the past few years, new template matching algorithms for multiple rotated templates have been proposed using the Karhune-Loeve (K-L) transform [5,6], and Fourier and K-L decomposition [7]. In their methods, the K-L transform is first applied to a set of rotated templates, and eigenvectors are extracted from them. Each template in the training set is approximated by a linear combination of salient eigenvectors. Normalized correlation

between rotated templates and the input image is then computed by substituting the approximations for the templates.

Matched filtering approaches using Gabor filters and wavelets [8,9,10] are popular alternatives in recent years for detecting objects in complicated images. However, they generally require significant amount of computation, and are of limited use because each view of the object may require a unique filter.

Existing template matching algorithms generally focus on detecting objects in gray-level images. Chromatic information of object patterns is not fully utilized to enhance the discrimination. Since color images contain more information per pixel than gray-level ones, color machine vision has been an active field during the last few years in pattern recognition applications. A simple and effective recognition scheme is to represent and match images on the basis of color histograms. Swain and Ballard [11] have proposed a color indexing method based on matching of color histograms for image retrieval. Gevers and Smeulders [12] analyze and evaluate various color models for the purpose of recognition of multicolored objects in the changes of illumination. In their experiment, reference objects are recorded in isolation (one per image) against a simple white cardboard background. The color indexing method is used to measure the similarity.

Mehtre *et al.* [13] propose the reference color table method for image retrieval. The method defines a table of reference colors, which contains a set of pre-selected color classes. In the matching process, each pixel in the color image is assigned to its nearest color class in the table, and the distance measure is used to compute the similarity based on the histogram of the newly assigned color classes. Kankanhalli *et al.* [14,15] use unsupervised clustering algorithms to determine the color classes so

that *a priori* knowledge is not necessary to set up the reference color table. Existing color-image matching algorithms basically use only color information from the color histogram of an image without utilizing spatial information of the object pattern. Those approaches may be suitable for image retrieval applications or detecting colored objects in a simple background. They possibly generate false match for colored objects in complex images.

Our work has been motivated by a need to develop an efficient color matching technique so that the detection of colored objects in a complex background can be effective and fast. For solving the problem of arbitrary orientation, we propose a rotation-invariant representation of colored patterns based on the color ring-projection transformation. Color ring-projection transforms the 2-D color image contained in a circular window into 1-D color signals as a function of radius. The color features of each ring with a specific radius are represented by the mean RGB tristimulus values of all pixels falling on the ring. The proposed matching process involves two phases. Phase I rapidly selects the most likely regions of a reference template in the scene image by computing the normalized correlation of color ring-projection patterns between them. Since the color ring-projection representation preserves only partial spatial information of the original 2-D image pattern, phase II then verifies the candidate locations selected in phase I by measuring the normalized correlation between the reference template and the candidate regions using the pixel-to-pixel template matching. In order to make the pixel-to-pixel matching rotation-invariant, we propose a new estimation scheme to determine the orientation of a colored pattern. We can simply rotate the reference template so that it aligns itself with the degree of rotation in the scene image. Therefore, the pixel-to-pixel matching in phase II is only computed for a few candidate locations, each in a specific orientation. This results in significant saving of computational time.

This paper is organized as follows: Section 2 first describes the proposed color ring-projection representation of colored objects, and the similarity measure of normalized correlation. Then the estimation of colored-object orientation is presented, and the normalized correlation of pixel-to-pixel template matching in color images is defined. The estimation accuracy of rotational angles is evaluated based on the experimental results of five colored test samples. Section 3 presents the experimental results for evaluating the efficacy of the proposed pattern matching algorithm. The paper is concluded in Section 4.

2. COLOR PATTERN MATCHING

2.1 Color Ring-Projection

Pattern matching basically involves two tasks: pattern representation followed by a matching process based on some similarity measures. In order to reduce the computational burden in the matching process, a new color ring-projection is proposed. It transforms a 2-D color image into a rotation-invariant representation in the 1-D ring projection space. The proposed transformation scheme for colored patterns is inspired by the ring projection algorithm [16,17], which is originally developed for character recognition in binary images.

Color provides powerful information for pattern matching. The color of a pixel is typically represented with the RGB tristimulus values, each corresponding to the red (R), green (G) and blue (B) frequency bands of the visible light spectrum. Images in the RGB color model consist of three independent color planes. The color

ring-projection transformation is carried out separately in each of the three primary-color planes. Let $R(x,y)$, $G(x,y)$ and $B(x,y)$ denote the R, G and B stimulus values at pixel coordinates (x,y), respectively. The pattern of interest is contained in a circular window of radius W. The radius chosen for the window depends on the size of the reference template. The color ring-projection of image plane $R(x,y)$ is given as follows. First, $R(x,y)$ in the Cartesian coordinates is transformed into the polar coordinates :

$$\begin{cases} x = r\cos\theta \\ y = r\sin\theta \end{cases}$$

Hence, $R(x,y) = R(r\cos\theta, r\sin\theta)$. The color ring-projection of image $R(x,y)$ at radius r, denoted by $p_R(r)$, is defined as the mean value of $R(r\cos\theta, r\sin\theta)$ at the specific radius r. That is,

$$p_R(r) = \frac{1}{2\pi r}\int_0^{2\pi} R(r\cos\theta, r\sin\theta)d\theta$$

Taking the mean of stimulus values for each specific ring reduces the effect of noise. The discrete representation of $p_R(r)$ in a search window of radius W is given by

$$p_R(r) = \frac{1}{n_r}\sum_k R(r\cos\theta_k, r\sin\theta_k) \qquad (1)$$

where n_r is the total number of pixels falling on the circle of radius r, $r = 0,1,2,\ldots,W$. The color ring-projections $p_G(r)$ and $p_B(r)$ of image planes $G(x,y)$ and $B(x,y)$ are defined in a similar way as $p_R(r)$, i.e.,

$$p_G(r) = \frac{1}{n_r}\sum_k G(r\cos\theta_k, r\sin\theta_k) \qquad (2)$$

$$p_B(r) = \frac{1}{n_r}\sum_k B(r\cos\theta_k, r\sin\theta_k) \qquad (3)$$

for $r = 0,1,2,\ldots,W$. Therefore, a 2-D image with two independent variables x and y in

each color plane is now represented by the 1-D ring-projection pattern with one single variable *r*. Since the projection is constructed along circular rings of increasing radii, the derived 1-D color ring-projection pattern is invariant to the rotation of its original 2-D image pattern. Figures 1(a) and 1(b) show the color images of a snail in two distinct orientations. Figures 1(c) - 1(h) present the plots of ring projections of three color planes as a function of radius *r*. It can be seen from the figures that the plots of ring projections are approximately identical, regardless of orientation changes. An original 2-D RGB image can now be represented by a sequence of RGB ring-projection vectors $\vec{P}(r) = \langle p_R(r), p_G(r), p_B(r) \rangle$, for $r = 0,1,2,\ldots,W$.

In the matching phase, the measure of similarity is given by the normalized correlation. Let

$$\vec{P}_M(r) = \langle p_R(r), p_G(r), p_B(r) \rangle$$

$$\vec{P}_S(r) = \langle \hat{p}_R(r), \hat{p}_G(r), \hat{p}_B(r) \rangle$$

$\vec{P}_M(r)$ and $\vec{P}_S(r)$ denote the RGB ring-projection vectors of the reference template and a scene subimage, respectively, at the ring of radius *r*, $r = 0,1,2,\ldots,W$, where *W* is the radius of the search window. The elements of both $\vec{P}_M(r)$ and $\vec{P}_S(r)$ are calculated from eqs. (1)-(3). The normalized correlation between two color ring-projection sequences $\{ \vec{P}_M(r) \mid r = 0,1,2,...,W \}$ and $\{ \vec{P}_S(r) \mid r = 0,1,2,...,W \}$ is defined by

$$\delta_p = \frac{\sum_{r=0}^{W} \sum_{i=R,G,B} \left[p_i(r) - \mu_p\right] \cdot \left[\hat{p}_i(r) - \hat{\mu}_p\right]}{\left\{\sum_{r=0}^{W} \sum_{i=R,G,B} \left[p_i(r) - \mu_p\right]^2 \sum_{r=0}^{W} \sum_{i=R,G,B} \left[\hat{p}_i(r) - \hat{\mu}_p\right]^2\right\}^{\frac{1}{2}}}$$

$$= \frac{\sum_{r=0}^{W} \left[\vec{P}_M(r) \bullet \vec{P}_S(r)\right] - 3(W+1)\mu_p \hat{\mu}_p}{\sqrt{\sigma_p^{2} \cdot \hat{\sigma}_p^{2}}} \tag{4}$$

where $\mu_p = \frac{1}{3(W+1)} \sum_{r=0}^{W} \left[p_R(r) + p_G(r) + p_B(r)\right]$

$$\hat{\mu}_p = \frac{1}{3(W+1)} \sum_{r=0}^{W} \left[\hat{p}_R(r) + \hat{p}_G(r) + \hat{p}_B(r)\right]$$

$$\sigma_p^{2} = \sum_{r=0}^{W} \left[p_R^{2}(r) + p_G^{2} + p_G^{2}(r)\right] - 3(W+1)\mu_p^2$$

$$\hat{\sigma}_p^{2} = \sum \left[\hat{p}_R^{2}(r) + \hat{p}_G^{2} + \hat{p}_G^{2}(r)\right] - 3(W+1)\hat{\mu}_p^2$$

$\vec{P}_M(r) \bullet \vec{P}_S(r)$ is the inner product of $\vec{P}_M(r)$ and $\vec{P}_S(r)$.

Here μ_p and $\hat{\mu}_p$ are the average values of the reference template and the scene subimage, respectively. σ_p^{2} and $\hat{\sigma}_p^{2}$ are associated with the variances of the template and the scene subimage. Normalized correlation between the reference template and a rotated scene subimage is efficiently computed by substituting the 1-D ring-projection pattern for the original 2-D pixel-image. The computational complexity is significantly reduced from $O(W^2)$ in 2-D images to $O(W)$ in the 1-D ring-projection space. The normalized correlation δ_p is between -1 and 1, and a perfect match of two identical patterns will have the maximum value of unity.

2.2 Pixel-to-Pixel Matching with the Estimated Orientation

The normalized correlation δ_p defined in eq. (4) is initially used in the matching process to select the best-matched candidates. Since the 1-D color ring-projection representation does not sufficiently preserve the spatial information of the original 2-D color image, the locations of the selected candidates in the matching phase are verified using the pixel-to-pixel template matching. Let

$$\overset{\mathrm{v}}{C}_M(i,j) = \langle R(i,j), G(i,j), B(i,j) \rangle$$

$$\overset{\mathrm{V}}{C}_S(x,y) = \langle \hat{R}(x,y), \hat{G}(x,y), \hat{B}(x,y) \rangle$$

$\overset{\mathrm{v}}{C}_M(i,j)$ and $\overset{\mathrm{v}}{C}_S(x,y)$ represent, respectively, the original RGB images of the reference template and a scene subimage contained in a circular window of radius *W*, where the elements of $\overset{\mathrm{v}}{C}_M(i,j)$ and $\overset{\mathrm{v}}{C}_S(x,y)$ are the R, G and B tristimulus values of a pixel. The normalized correlation between two RGB images

$$\{\overset{\mathrm{v}}{C}_M(i,j) \mid i^2 + j^2 \le W\} \quad \text{and} \quad \{\overset{\mathrm{v}}{C}_S(x+i, y+j) \mid i^2 + j^2 \le W\}$$

is given by

$$\delta_c = \frac{\sum_{j=-v}^{v}\sum_{i=-w}^{w}\left[\overset{\mathrm{V}}{C}_M(i,j) \bullet \overset{\mathrm{V}}{C}_S(x+i, y+j)\right] - 3N_c\mu_c\hat{\mu}_c}{\sqrt{\sigma_c^{2} \;\; \hat{\sigma}_c^{2}}} \tag{5}$$

where $\mu_c = \frac{1}{3N_c}\sum_{j=-v}^{v}\sum_{i=-w}^{w}\left[R(i,j) + G(i,j) + B(i,j)\right]$

$$\hat{\mu}_c = \frac{1}{3N_c}\sum_{j=-v}^{v}\sum_{i=-w}^{w}\left[\hat{R}(x+i, y+j) + \hat{G}(x+i, y+j) + \hat{B}(x+i, y+j)\right]$$

$$\sigma_c = \sum_{j=-v}^{v}\sum_{i=-w}^{w}\left\{\left[R(i,j)\right]^2 + \left[G(i,j)\right]^2 + \left[B(i,j)\right]^2\right\} - 3N_c\mu_c^{\,2}$$

$$\hat{\sigma}_c = \sum_{j=-v}^{v}\sum_{i=-w}^{w}\left\{\left[\hat{R}(x+i,y+j)\right]^2 + \left[\hat{G}(x+i,y+j)\right]^2 + \left[\hat{B}(x+i,y+j)\right]^2\right\} - 3N_c\hat{\mu}_c{}^2$$

$$v = \sqrt{W^2 - i^2}$$

N_c = the total number of pixels in the circular window.

The value of pixel-based correlation δ_c is also between -1 and 1, and the perfect match will have a maximum value of unity. Since the correlation δ_c computes the color information based on the 2-D spatial location of each pixel in the image, the resulting correlation coefficient is sensitive to orientation changes. If a clue regarding rotation can be extracted from the input subimage $\left\{\vec{C}_S(x,y)\right\}$, then simply rotate the template $\left\{\vec{C}_M(i,j)\right\}$ so that it aligns itself with the degree of rotation in $\left\{\vec{C}_S(x,y)\right\}$. This normalization for rotation avoids exhaustive rotations of the template to look for the best match.

In binary images, the orientation of an object can be easily determined from the principal axes (eigenvectors) of the covariance matrix of the pixel coordinates [4]. In color images, the orientation of a colored pattern is difficult to define. Pixels with different color values in color images can be considered as particles with different densities in physical objects. Then the usual practice in physics is to choose the axis of least second moment [18] as the object direction. We find the line for which the integral of the square of the distance to points in the object is a minimum

$$E = \int\int d^2\rho(x,y)dxdy$$

where d is the perpendicular distance from the point (x,y) to the line sough after, and $\rho(x,y)$ is the density at (x,y). By minimizing E, we can obtain the orientation θ of

the line [18]:

$$\theta = \frac{1}{2}\tan^{-1}\left(\frac{b}{a-c}\right) \tag{6}$$

where $a = \sum_{y'}\sum_{x'}(x')^2\rho(x',y')$

$b = 2\sum_{y'}\sum_{x'}(x'\cdot y')\rho(x',y')$

$c = \sum_{y'}\sum_{x'}(y')^2\rho(x',y')$

(x',y') are the shifted coordinates with the origin (0,0) at the center of the search window.

For an object in the binary image, the density $\rho(x',y')$ is uniform, and is simply given by the binary gray-value of pixels. In color images, the value of a color feature can be used to represent the density $\rho(x',y')$ of each pixel in the search window. In this study, we simply select one salient color feature derived from various color models, and then normalize the value of the color feature that sums to unity for all pixels in the search window to represent the density of a colored pixel. We consider two popular color models HSI and CIELAB [4,19] to obtain various color features. The conversion from the RGB space to the HSI space is given by

$$I = \frac{1}{3}(R+G+B)$$

$$S = 1 - \frac{3}{(R+G+B)}\left[\min(R,G,B)\right]$$

$$H = \cos^{-1}\left\{\frac{\frac{1}{2}\left[(R-G)+(R-B)\right]}{\left[(R-G)^2+(R-B)^2+(G-B)^2\right]^{1/2}}\right\}$$

If $(B/I) > (G/I)$, then $H = 360^{\circ} - H$.

Here color features I, S and H represent intensity, saturation and hue of a color, respectively.

The CIELAB color space is an international standard, which corresponds to human color perception and very closely resembles uniform color space. The CIELAB space requires an intermediate transform to the XYZ space from the system dependent RGB space. The transform for NTSC color vision sensor is

$$\begin{bmatrix} X \\ Y \\ Z \end{bmatrix} = \begin{bmatrix} 0.607 & 0.174 & 0.200 \\ 0.299 & 0.587 & 0.114 \\ 0.000 & 0.066 & 1.116 \end{bmatrix} \begin{bmatrix} R \\ G \\ B \end{bmatrix}$$

The CIELAB equation is then applied for tristimulus values *X*, *Y* and *Z*:

$$L* = 116\left(\frac{Y}{Y_n}\right)^{1/3} - 16$$

$$a* = 500\left[\left(\frac{X}{X_n}\right)^{1/3} - \left(\frac{Y}{Y_n}\right)^{1/3}\right]$$

$$b* = 200\left[\left(\frac{Y}{Y_n}\right)^{1/3} - \left(\frac{Z}{Z_n}\right)^{1/3}\right]$$

where X_n, Y_n and Z_n are the tristimulus values of the reference white. L^* is a correlate to perceived lightness. The $a*$ and $b*$ dimensions correlate approximately with red-green and yellow-blue chroma perceptions. The CIELAB color space can also be represented in terms of cylindrical coordinates, which provide predictors of chroma C^*_{ab} and hue h_{ab} as expressed below :

$$C^*_{ab} = (a^2* + b^2*)^{1/2}$$

$$h_{ab} = \tan^{-1}\left(b* / a*\right)$$

Given a color feature $f_c(x, y)$, where

$$f_c(x, y) \in \left\{H,\ S,\ I,\ L*,\ a*,\ b*,\ h_{ab},\ C^*_{ab}\right\}$$

the density $\rho(x, y)$ at pixel (*x,y*) is defined by

$$\rho(x,y) = \frac{f_c(x,y)}{\sum_{(i,j)\in W_c} f_c(i,j)}$$

for all (x,y) contained within the search window W_c. The gray value of a pixel in its corresponding gray-level image is also considered as one of the color features so that the performance of the density representation in both color images and gray-scale images can be evaluated in the experiment.

Figures 2(a) - 2(e) show five test samples used in this study for evaluating the angular accuracy of the proposed orientation estimator. Each test sample is contained in a circular window of radius 25 pixels, with eight-bit intensity per color band. Also, each test sample is synthetically rotated from 0° to 360° in 1° increment so that the estimated orientations can be compared with the actual ones. A total of 360 rotated images is created for each of the five test samples. Table 1 summarizes means, standard deviations and maximum values of the angular errors of the estimated orientations. It can be seen from Table 1 that color feature $a*$ derived from the CIELAB space gives the best overall performance. The mean angular error of orientation is less than 5°, and the standard deviation is smaller than 2.7°. The maximum angular error in 1, 800 (360 orientations $\times$ 5 test samples) images is only 8°.

The gray values in gray-level images perform unstably for the five test samples. Color feature *S* derived from the HSI space works poorly for the test samples shown in Figures 2(b), 2(c) and 2(e), and their resultant statistics are not included in Table1. Color feature H from the HSI space gives the mean angular error less than 7°. However, it yields the maximum angular error of 18° and the standard deviation as large as 5.3°. It is unstable for angular estimation. Compared with the exhaustive matching of the reference template in all possible orientations, the proposed

pixel-to-pixel template matching in the verification phase can be calculated efficiently by searching only the neighborhood of the estimated orientation. Based on our empirical study, search angles between -5° and 5° in the vicinity of the estimated orientation is generally sufficient to reach the best match with the use of color feature a^*.

3. EXPERIMENTAL RESULTS

In this section, we present the experimental results for evaluating the efficacy of the proposed color pattern matching method. In our implementations, all algorithms are programmed in the C language and executed on a personal computer with a Pentium 300 MHz processor. The effective image size is 256×256 pixels with eight bits of intensity per color band.

In order to evaluate the effect of rotation changes, two test samples shown in Figures 3(a) and 4(a) are rotated in two distinct orientations as shown in Figures 3(b1) - 3(c1) and 4(b1) - 4(c1). The patterns marked by yellow circles in Figures 3(a) and 4(a) are used as reference templates. The five largest correlation coefficients δ_p derived from the color ring-projection matching are marked by circles of colors red, green, blue, yellow and indigo in their descending order. Figure 3(a) shows an image that contains many small objects similar in shapes and colors. Figures 3(b1) and 3(c1) present the candidate locations of the reference templates detected by the color ring-projection matching. Figures 3(b2) and 3(c2) display the verification results from the pixel-to-pixel template matching. Figure 4(a) shows the image containing many similar resistor components of different resistances (coded by different color stripes) in a complex background. The target resistor of $392\,\Omega$ placed in arbitrary locations and orientations is reliably detected in both scene images as shown in Figures 4(b2)

and 4(c2). Notice that the location with the largest correlation coefficient δ_p (marked by a red circle in Figures 3(b1),3(c1), 4(b1) and 4(c1)) obtained from the color ring-projection matching is coincident with the best match found in the pixel-to-pixel template matching for each of the two test samples. All instances of reference templates are correctly located, regardless of rotation changes.

Figures 5 and 6 show additional experimental results of detecting small parts on printed circuit boards (PCBs). Figure 5(a) presents the original image with the target component marked by a yellow circle. Figures 5(b) and 5(c) show that the target component is well located in color ring-projection and pixel-to-pixel matching phases, respectively. Notice that the scene image is rotated by 90° with respect to the original one, and the estimated orientation is 89°. In Figure 6(a), the target object is the solder pad labeled “R07” on the PCB, and is marked by a yellow circle in the image. Figure 6(b) shows the locations of the five largest correlation coefficients δ_p in the ring-projection matching phase. Figure 6(c) presents the best match verified by the pixel-to-pixel template matching. The scene image is a shifted version of the original one, and the estimated orientation is 1°. It can be seen from Figures 6(b) and 6(c) that the target object is well located as indicated by the red circles in the images. Figures 7 and 8 show the experiments that detect objects in more hostile environments. Figure 7 illustrates the detection result for objects in severely overexposed and underexposed images. Figure 8 presents the detection result for objects in different color backgrounds. It can be seen from both Figures 7 and 8 that the proposed method also works well for detecting objects in varying environment.

4. CONCLUSION

Template matching has been a fundamental technique in machine vision for detecting objects in complex images. One of the major limitations of traditional pixel-by-pixel template matching is that an enormous number of templates must be matched against an image field to account for changes in rotation of reference templates. Many existing template matching methods are mainly applied to gray-level images. They ignore the powerful color information and make the object detection task unreliable.

In this study, we have proposed a rotation-invariant template matching method for detecting objects in color images. The complexity and computation load of the correlation function method for detecting objects in arbitrary orientations are reduced significantly by the 1-D color ring-projection representation. It can rapidly select the possible locations of a reference template in the input scene by computing the normalized correlation of 1-D color ring-projection patterns. The candidate locations with high correlation coefficients obtained in the color ring-projection matching phase are then verified by the pixel-to-pixel template matching. To make the pixel-based matching invariant to rotation, the color feature $a*$ derived from the CIELAB space is used as pixel density, and the axis of least second moment is employed to estimate the rotational angle of the reference template. This alleviates the exhaustive search of unknown orientation in traditional template matching methods.

For an image of size $N \times N$, and a circular window of radius W, the computational complexity of the proposed color ring-projection matching is given by $O(W \cdot N^2)$ for objects in arbitrary orientations, compared with $O(W^2 \cdot N^2)$ of the traditional pixel-by-pixel template matching for objects in each possible orientation. The proposed pixel-to-pixel matching in the verification phase is only computed for a few

candidate locations in a specific orientation. Therefore, the proposed pattern matching scheme is efficient in computation using the rotation-invariant representation, and is robust in matching using the color information. Computational time of the proposed color ring-projection matching is 6 seconds on the Pentium 300 MHz personal computer for an arbitrarily-rotated image of size 256×256 pixels and a circular window of radius 25 pixels. For traditional template matching methods, computational time is 20 seconds for images in a fixed orientation. If the object orientation can be arbitrary, and the search angle ranges from 0° to 360° with 1° resolution, computational time of traditional methods will dramatically increase to 7,200 seconds.

REFERENCES

1. W. K. Pratt, Digital Image Processing, Wiley-Interscience, New York, N.Y., 1991.
2. S. Mori, C. Y. Suen and K. Yamamoto, Historical reviews of OCR research and development, Proceedings of the IEEE 80 (1992) 1029-1057.
3. M. Moganti and F. Ercal, Automatic PCB inspection algorithms: a survey, Computer Vision and Image Understanding 63 (1996) 287-313.
4. R. C. Gonzalez and R. E. Woods, Digital Image Processing, Addison-Wesley, Reading, Mass., 1992.
5. S. Yoshimura and T. Kanade, Fast template matching based on the normalized correlation by using multiresolution eigen-images," Proc. IROS'94, Munich, Germany, 1994.
6. O. Amidi, Y. Mesaki, T. Kanada and M. Uenohara, Research on an autonomous vision-guided helicopter, Proc. Fifth RI/SME World Conf. Robotics Research, Cambridge, Mass., 1994.
7. M. Uenohara and T. Kanada, Use of Fourier and Karhunen-Loeve decomposition for fast pattern matching with a large set of templates, IEEE Trans. Pattern Anal. Mach. Intell. 19 (1997) 891-898.
8. A. K. Jain, N. K. Ratha and S. Lakshmanan, Object detection using Gabor filters, Pattern Recognition 30 (1997) 295-309.
9. D. P. Casasent, J. -S. Smokelin and A. Ye, Wavelet and Gabor transforms for detection, Optical Engineering 31 (1992) 1893-1898.
10. R. N. Strickland and H. I. Hahn, Wavelet transform methods for object detection and recovery, IEEE Trans. Image Processing 6 (1997) 724-735.
11. M. J. Swain and D. H. Ballard, Color indexing, Intl. J. Computer Vision 7 (1991) 11-32.
12. T. Gevers and A. W. M. Smeulders, Color-based object recognition, Pattern Recognition 32 (1999) 453-464.
13. B. M. Mehtre, M. S. Kankanhalli, A. D. Narasimhalu and G. C. Man, Color matching for image retrieval, Pattern Recognition Letters 16 (1995) 325-331.
14. M. S. Kankanhalli, B. M. Mehtre and J. K. Wu, Cluster-based color matching for

image retrieval, Pattern Recognition 29 (1996) 701-708.

15. M. S. Kankanhalli, B. M. Mehtre and H. Y. Huang, Color and spatial feature for content-based image retrieval, Pattern Recognition Letters 20 (1999) 109-118.

16. Y. Y. Tang, H. D. Cheng and C. Y. Suen, Transformation-ring-projection (TRP) algorithm and its VLSI implementation, Int. J. Pattern Recogn. Artif. Intell. 5 (1991) 25-56.

17. P. C. Yuen, G. C. Feng and Y. Y. Tang, Printed Chinese character similarity measurement using ring projection and distance transform, Int. J. Pattern Recogn. Artif. Intell. 12 (1998) 209-221.

18. B. K. P. Horn, Robot Vision, The MIT Press, Cambridge, Mass., 1990.

19. M. D. Fairchild, Color Appearance Models, Addison-Wesley, Reading, Mass., 1998.

(a) Original image

(b) Rotated image

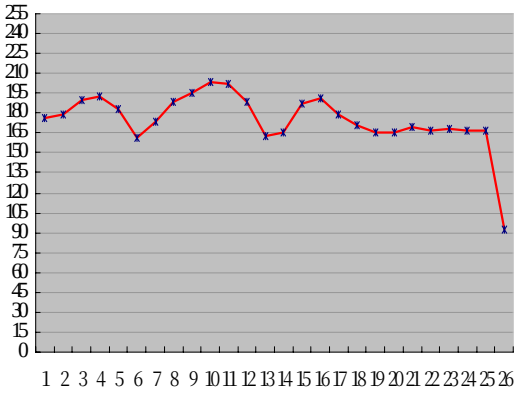

(c) $p_R(r)$ of $R(x,y)$ in (a)

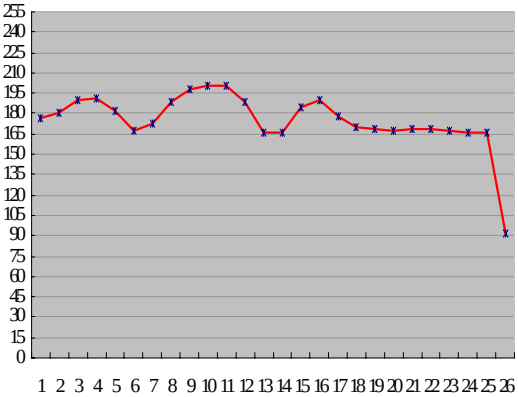

(d) $p_R(r)$ of $R(x,y)$ in (b)

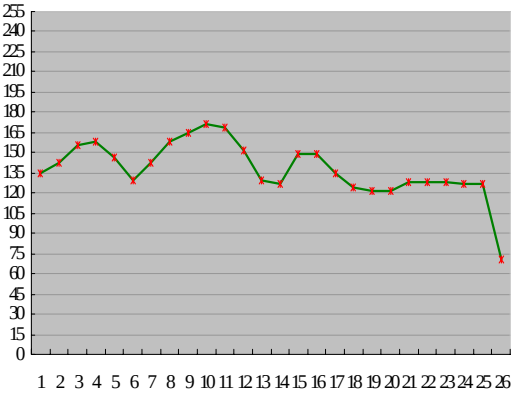

(e) $p_G(r)$ of $G(x,y)$ in (a)

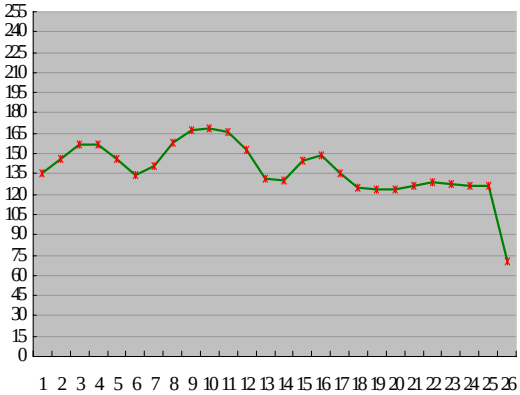

(f) $p_G(r)$ of $G(x,y)$ in (b)

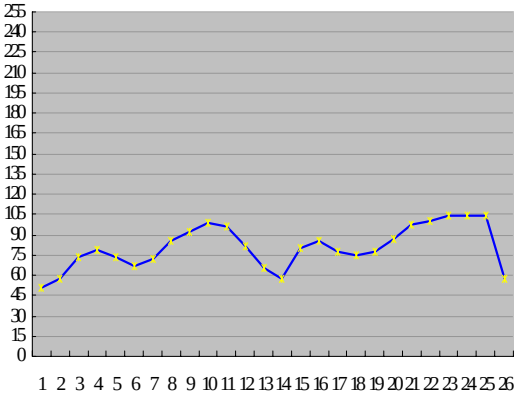

(g) $p_B(r)$ of $B(x,y)$ in

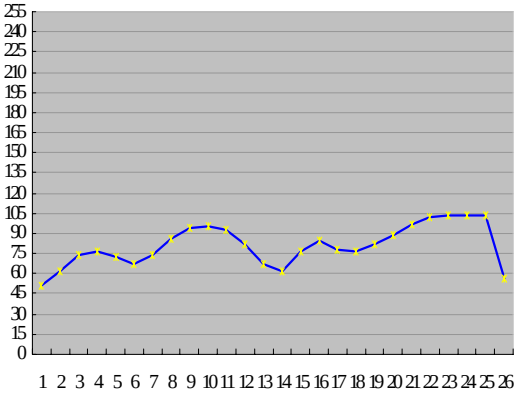

(h) $p_B(r)$ of $B(x,y)$ in (b)

Figure 1. Color ring-projection representation of a snail image in two distinct orientations.

(a) (b) (c) (d) (e)

Figure 2. Five test samples used for orientation estimation.

Table 1. Estimated rotational errors from various color features.

Test Sample	Statistics (degree)	Gray-level image	Color image							
			HSI			CIELAB				
		Gray level	H	S	I	L	a^*	b^*	C^*_{ab}	h_{ab}
Fig. 2(a)	Mean error	4.2	6.4	3.0	6.3	4.3	4.5	2.2	3.1	4.7
	Std. dev.	2.4	4.4	1.8	3.4	3.1	2.7	1.8	2.2	3.4
	Max. error	8	16	8	12	10	8	8	9	15
Fig. 2(b)	Mean error	1.1	3.7	-	1.7	2.7	2.4	7.7	3.1	7.9
	Std. dev.	0.7	2.9	-	1.1	2.6	1.9	4.9	1.7	3.8
	Max. error	2	11	-	4	8	6	15	8	13
Fig. 2(c)	Mean error	34.6	6.7	-	7.9	5.3	1.5	0.8	1.0	4.9
	Std. dev.	25.7	5.3	-	5.2	3.2	1.0	0.4	0.9	3.7
	Max. error	67	18	-	17	12	4	2	3	14
Fig. 2(d)	Mean error	13.0	3.8	3.8	2.0	5.6	0.8	5.6	9.3	6.3
	Std. dev.	9.8	2.2	2.8	1.2	5.0	0.7	2.9	7.0	4.5
	Max. error	32	7	10	4	16	2	11	24	14
Fig. 2(e)	Mean error	2.5	1.7	-	2.9	4.1	2.3	35.6	7.3	2.1
	Std. dev.	1.7	1.7	-	2.2	2.8	1.4	26.0	4.7	1.5
	Max. error	6	5	-	8	10	5	76	16	5

(a)

(b1)

(b2)

(c1)

(c2)

Figure 3. An image,which contains many similar objects, used to evaluate the effect of orientation changes: (a) the original color image (the reference template is marked by a yellow circle); (b1),(b2) the detection results from the matching phase (color ring-projection matching) and the verification phase (pixel-to-pixel matching), respectively, for one rotated image; (c1), (c2) the detection results from the matching phase and the verification phase for another rotated image.

(a)

(b1)

(b2)

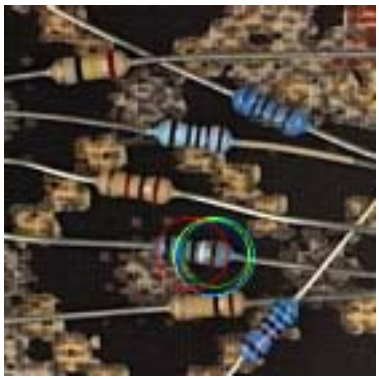

(c1)

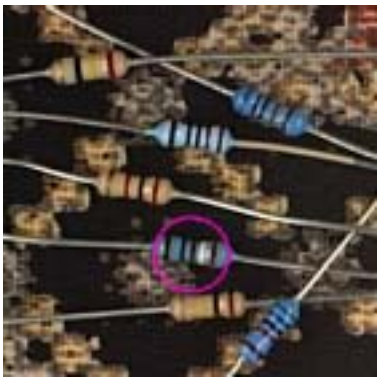

(c2)

Figure 4. A resistor image used to evaluate the effect of orientation changes: (a) the original color image (the reference template is marked by a yellow circle); (b1),(b2) the detection results from the matching phase (color ring-projection matching) and the verification phase (pixel-to-pixel matching), respectively, for one rotated image; (c1), (c2) the detection results from the matching phase and the verification phase for another rotated image.

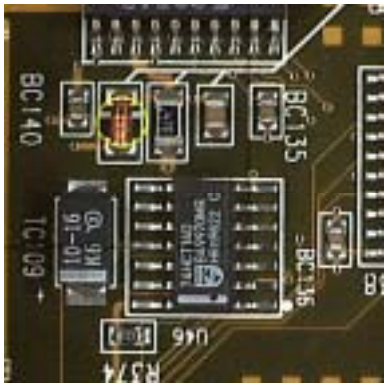

(a)

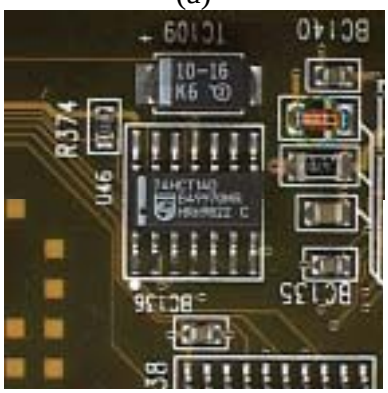

(b)

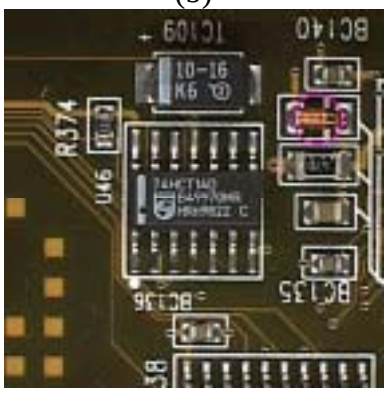

(c)

Figure 5. Detection of a resistor component on the PCB: (a) the original image; (b) the candidates with five largest correlation values obtained from the matching phase; (c) the best match verified.

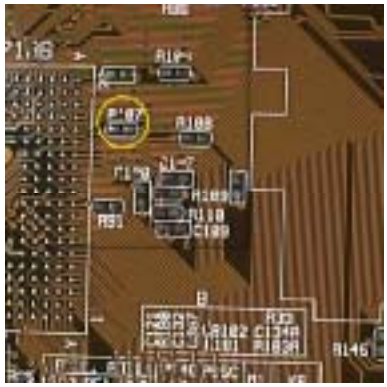

(a)

(b)

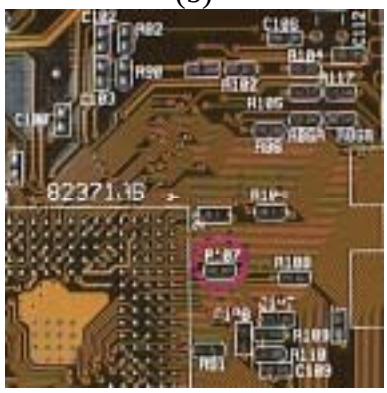

(c)

Figure 6. Detection of a solder pad labeled “R07”: (a) the original image; (b) the candidates with five largest correlation values obtained from the matching phase; (c) the best match verified.

(a)

(b)

(c)

Figure 7. Detection of an object in varying illumination : (a) the template image; (b) the overexposed image; (c) the underexposed image.

(a)

(b)

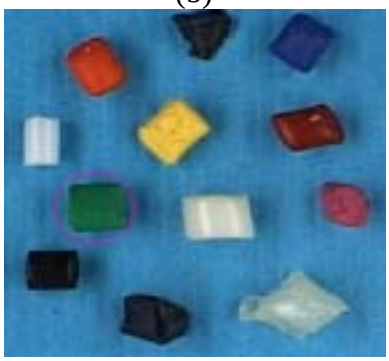

(c)

Figure 8. Detection of an object in varying background: (a) the template image; (b) the image with a yellow background; (c) the image with a blue background.